# Highly Efficient Photocatalytic Hydrogen Evolution Using a Self-Assembled Octupolar Molecular System

Hyun-Jun Lee,[a] Abasi Abudulimu,[b, c] Juan Carlos Roldao,[b, d] Hyunwoo Nam,[a] Johannes Gierschner,*[b] Larry Lüer,*[b, e] and Soo Young Park*[a, f]

A highly efficient photocatalytic hydrogen evolution system was prepared by using an octupolar molecule as a building block of self-assembled nanoparticles. The photocatalytic system showed an enhanced hydrogen evolution reaction (HER) rate upon the addition of halide ions, which was attributed to an external heavy atom effect enhancing intersystem crossing. The HER rate of the photocatalytic system was proportional to the atomic weight and concentration of halide ion additives, and its maximum HER rate reached 460 mmol/g·h in the presence of iodide ions and a metal co-catalyst. Further, the photocatalytic system without any halide ion additives generated hydrogen gas utilizing seawater and stimulated sunlight with remarkable efficiency (apparent quantum yield ~ 3.8 %).

## Introduction

In the last few decades, the development of photocatalytic water-splitting systems has been a major focus to produce hydrogen gas on a commercial scale.[1] For example, metal complexes[2] or metal co-catalyst-decorated inorganic semiconductors have shown an impressive hydrogen evolution reaction (HER, apparent quantum yield, AQY ~ 1 at ultraviolet region),[3] but a limited visible light absorption. But unlike inorganic materials, organic materials have the advantage of having an easily tunable band gap; therefore, to better utilize solar light, photocatalytic systems using organic semiconducting materials have been reported in the last years.[4] So far, systems such as polymeric materials[5] and covalent organic frameworks (COFs)[6] have been demonstrated with promising performances, (HER rate ~ 6 mmol/g·h for polymer,[5c] 30 mmol/g·h for COF[6e]) but they usually have low water-compatibilities due to their hydrophobicity. Furthermore, reproducibility remains a problem because of the challenges in controlling size and molecular weight of the particles.[7] Other concepts, such as self-assembled nanoparticles consisting of amphiphilic organic building blocks, have also been reported recently.[8] These self-assembled nanoparticles made by bottom-up approaches usually have good water compatibilities and ease of structural control by designing their building block molecules. Although these self-assembled nanoparticles are promising candidates for the next generation of organic photocatalysts, their activities still remain low (11.7 mmol/g·h).[8g,9] Besides, photocatalytic system based on self-assembled nanoparticles are yet to be developed, as only few building blocks like perylene imides[8b,d,g] or porphyrins[8e,10] were reported by now. Moreover, an inherent limitation of organic semiconducting materials as photocatalysts is their typically fast excited state decay rate and strong exciton binding energies hampering the photo-induced electron transfer (PeT). Many researchers have explored new ways to overcome this weakness; for instance by the introduction of donor-acceptor type heterojunctions in polymeric systems[11] or by enabling intimate H-aggregation in self-assembled molecular systems.[8b,12] In a previous work,[8c] we originally proposed the use of triplet exciton of the photosensitizer to extend the exciton lifetime of the self-assembled organic material, giving the system more opportunities to run the desired photocatalytic cycle. However, such self-assembled systems are yet to be designed elaborately for the improved visible light absorption and HER activity.[8c]

Here, we used two innovative strategies to develop a highly efficient and stable self-assembled photocatalytic system. For

[a] Dr. H.-J. Lee, H. Nam, Prof. Dr. S. Y. Park
Center for Supramolecular Optoelectronic Materials
Department of Materials Science and Engineering
Seoul National University
Seoul 151–742 (Korea)
E-mail: Parksy@snu.ac.kr
[b] Dr. A. Abudulimu, J. C. Roldao, Prof. Dr. J. Gierschner, Prof. Dr. L. Lüer
Madrid Institute for Advanced Studies
IMDEA Nanoscience, C/ Faraday 9
Ciudad Universitaria de Cantoblanco
28049 Madrid (Spain)
E-mail: johannes.gierschner@imdea.org
larry.lueer@fau.de
[c] Dr. A. Abudulimu
Current Address:
Wright Center for Photovoltaics Innovation and Commercialization (PVIC)
Department of Physics and Astronomy
The University of Toledo
Toledo, OH 43606 (USA)
[d] J. C. Roldao
Current Address:
Donostia International Physics Center, DIPC
20018 Donostia, Euskadi (Spain)
[e] Prof. Dr. L. Lüer
Current Address:
Institute of Materials for Electronics and Energy Technology (i-MEET)
Friedrich-Alexander-Universität Erlangen-Nürnberg
Martensstrasse 7, 91058 Erlangen (Germany)
[f] Prof. Dr. S. Y. Park
Research Institute of Advanced Materials (RIAM)
Seoul National University
08826 Seoul (Korea)

Supporting information for this article is available on the WWW under https://doi.org/10.1002/cptc.202200177

this, we designed and synthesized a novel octupolar molecule with excellent visible light absorption and strong intramolecular charge transfer (CT) characteristics. Octupolar molecules were extensively explored as two photon absorption medium due to their large hyperpolarizabilities.[13] Three-fold symmetric octupolar molecules were indeed reported as a building block of efficient COF HER catalyst (2.52 mmol/g·h); this octupolar COF consisted of electron donor-π-acceptor structure exhibiting excellent light absorption and charge separation.[14] Furthermore, we adopted external heavy atoms to restrict unwanted singlet recombination: various halogen ions were utilized to enhance intersystem crossing (ISC) in the excited state manifold. This strategy effectively suppressed unwanted pathways (non-radiative decay of polaron state), promoting the desired photocatalytic hydrogen evolution cycle. With iodide ion and metal co-catalysts, HER rate and AQY reached up to 460 mmol/g·h (Figure S12A) and 9.8% at 500 nm, respectively; furthermore, the building block, including organic parts, operated in the photocatalytic cycle about 20,000 times during two days under visible light irradiation. Not only iodide, but also bromide and chloride ions enhanced HER performance; however less effectively. Based on this, we could successfully demonstrate a seawater-based HER system. Additionally, our analysis of the photocatalytic mechanism in this work provided clear evidence for the role of additives, that is metal co-catalysts and halogen ions. Our system provides the highest HER rate of self-assembled photocatalytic systems reported so far, and may provide important molecular design rule for efficient organic hydrogen evolution systems.

## Results and Discussion

We designed a novel octupolar molecule, ((4,4′,4′′-(((1Z,1′Z,1′′Z)-(nitrilotris(benzene-4,1-diyl))tris(1-cyanoethene-2,1-diyl))tris(benzene-4,1-diyl))tris(1-methylpyridin-1-ium)), as a building block for the self-assembled photocatalytic hydrogen evolution system. (Figure 1A) The octupolar molecule was designed based on a thorough strategy to obtain excellent photo-induced activity.[13–14] The molecule provides a triphenylamine moiety in its core, which was also reported as an efficient donor moiety for octupolar molecules.[13d] Three electron accepting and hydrophilic pyridinium groups were connected to the central donor moiety via cyanovinylene bridges; the latter were designed to assist charge separation with its strong electron accepting characteristics.[13d] The octupolar nature is evident from the natural transition orbital topologies of the lowest excited state, as seen in the time-dependent density functional theory (TD-DFT) analysis of Figure S14 in the Supporting Information. In aqueous solution, the octupolar building blocks formed a self-assembled structure according to the appropriate balance between the hydrophobic core and the hydrophilic arms. The average (hydrodynamic) diameter of self-assembled nanoparticles was about 145 nm in dynamic light scattering (DLS, Figure S1) measurement, and the zeta potential of the self-assembled structure was +38 mV in electrophoretic light scattering (ELS) measurements. During the photo-reduction process, the metal co-catalyst grew on the surface of the self-assembled nanoparticles. This allows for rapid electron transfer from the supramolecular system to the metal co-catalyst, enhancing the hydrogen production performance. The positive zeta-potential of the self-assembled nanoparticles also affected the HER performance by enabling effective interaction with negatively charged halide additives[8c,15] or Pt colloids which have negative zeta-potential.[16] The self-assembled molecular photocatalytic system was stable during the photocatalytic hydrogen reduction cycle, and the self-assembled structures were still observed in the dried film in the TEM images in Figure 1B, 24 hours after operating duration of more than 10,000 times on average, as represented by the turnover number (TON). The HRTEM image in Figure 1B further evidences the presence of crystalline Pt co-catalyst colloids on the surface of the amorphous organic aggregates. Much like metal co-catalysts decorated on inorganic semiconductors,[17] Pt nanoparticles on the self-assembled nanoparticles should effectively receive electrons from photo-active organic parts to run the HER. Specifically, the apparent quantum yield (AQY) of hydrogen production followed the strength of light absorption of the building block molecule; in fact, the maximum AQY (9.8% at 500 nm, Figure 1C) was observed in the spectral region with the highest absorbance, while it decreased at wavelengths with low absorbance. This confirmed that controlling the charge-transfer characteristics and π-conjugation of the octupolar molecule indeed affects the performance of the photocatalytic system.

Additives were used to improve the performance of the photocatalytic system. Pt was used as a co-catalyst, and sodium halides were added to improve the performance. In fact, without additives, the HER rate was finite but negligible, whereas with 0.15 M of iodide, an HER rate of about 8 mmol/g·h was achieved; upon extra addition of 0.5 μmol of Pt, an HER rate of about 350 mmol/g·h (Figure S12A) was obtained. As a result, interestingly, both TOF (turnover frequency) and TON increased dramatically upon addition of the Pt co-catalyst and halogen ions, evidently by controlling post-photoexcitation steps. In our previous study, we demonstrated a moderately efficient, self-assembled photocatalytic system consisting of three-fold symmetric but *non-octupolar* molecules by utilizing the triplet state of an external photosensitizer,[8c] which is limited by poor visible light absorption. Herein, we synthesized novel self-assembled *octupolar* molecular photocatalytic system with adequate bandgap (2.2 eV) to utilize solar energy, and give direct evidence for the role of important additives (halides and metal co-catalysts). To investigate the role of the octupolar molecule's triplet state in increasing the HER performance of the photocatalytic system, we first measured the HER rate dependence on the external heavy atom effect as shown in Figure 1D. Namely, both TOF and TON of the supramolecular photocatalysts showed a large enhancement with increasing atomic weight of the added halides (Figure 1D). From this unambiguous relationship, it can be seen that increasing the ISC by addition of an external heavy atom salt has a decisive effect on the hydrogen production performance. This evidences, as pointed out in many photocatalytic systems,[18] that the

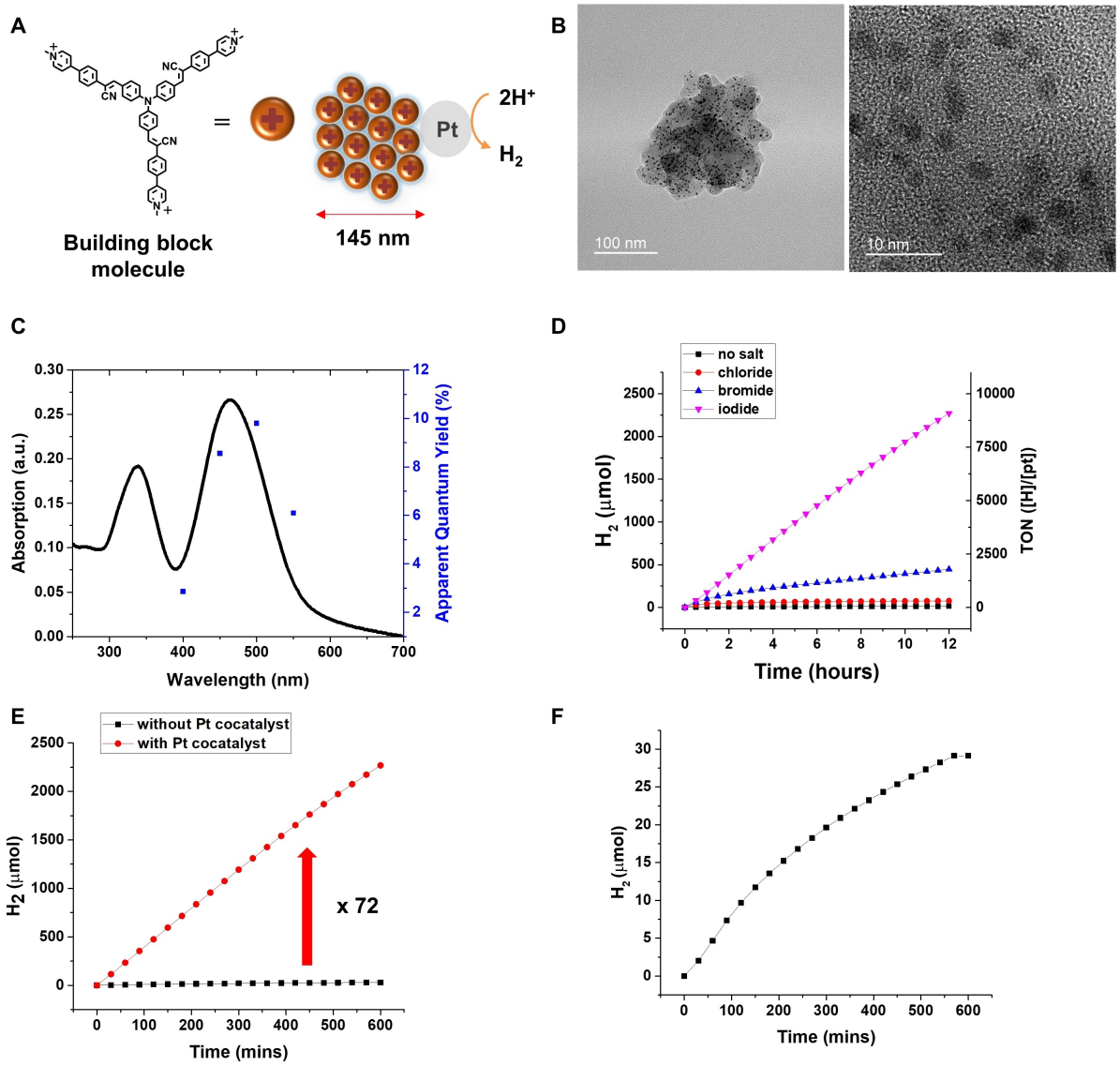


**Figure 1.** (A) Molecular structure of the building block and scheme of the self-assembled molecular photocatalytic system. (B) TEM and HRTEM images of the supramolecular system after 24 hours of photocatalytic reaction. (C) UV/Vis absorption spectrum of the self-assembled molecular system and apparent quantum yield (AQY) for hydrogen evolution versus excitation wavelength. (D) HER rate change of the self-assembled molecular system upon addition of halide ions. (E) HER rate change of the self-assembled molecular system upon addition of Pt co-catalyst. (F) Expanded graph of sample 'without Pt cocatalyst' in (E).

use of triplet states with much longer lifetime than the singlet state is actually beneficial in our self-assembled molecular photocatalytic hydrogen evolution system as well. This observation thus suggests that the ISC from the singlet to the triplet state in the octupolar molecule is a rate determining step for the final electron transfer reaction from octupolar molecule to Pt (Scheme 1). To further support this premise, we carried out Transient Absorption (TA) spectroscopy, singlet oxygen formation experiments (Figure S2) and Raman scattering measurements (Figure S3).

### Transient absorption (TA) spectroscopy

The excited-state dynamics of the building block molecule was explored by TA spectroscopy, which also revealed the role of halide salt additives. Due to severe scattering observed in the aqueous solution of the nanoparticles (Figure S16), we instead used other polar solvent, dimethylsulfoxide (DMSO). In DMSO solution, color change upon nanoparticle formation appeared at lower concentration (between 0.01 mM and 0.1 mM, Figure S17). As a result, we could analyze the dynamics of the photoexcited nanoparticles via TA spectroscopy experiments in DMSO solution. Figure 2 shows normalized TA spectra of the nanoparticles in the presence of NaCl (panels A,B), NaBr (panels C,D), and NaI (panels E,F). All TA spectra show a strong photoinduced absorption band at around 2.15 eV, which forms

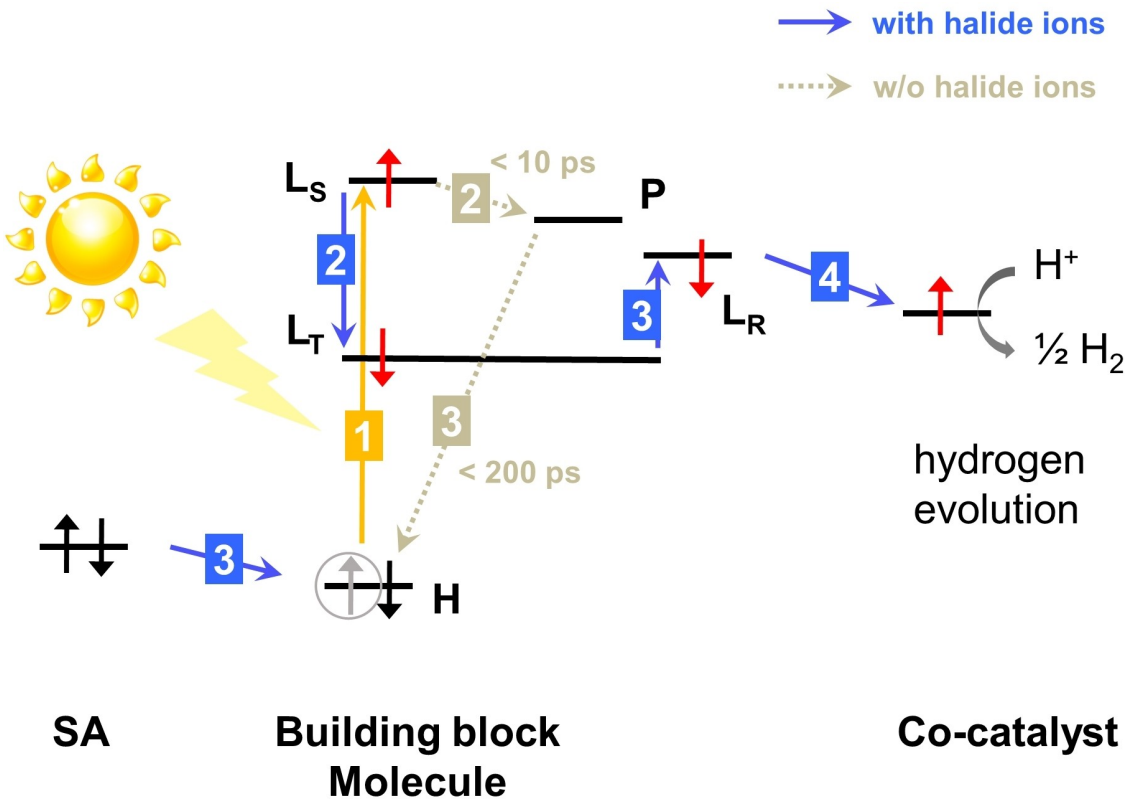


**Scheme 1.** Proposed reaction scheme of the self-assembled molecular photocatalytic system derived from TAS experiments. ($L_S$, $L_T$, $L_R$ and P denote singlet excited state, triplet excited state, reduced state and polaron state, respectively).

within 3 ps from the primary photoexcitation. The observation of the delayed formation of this band and the spectral coincidence with the absorption spectrum of the reduced nanoparticles (i.e. at ca. 600 nm, from photoelectrochemistry, see Figure S6 and the discussion on 'stability' further down) leads us to assign this band to a polaron state of the nanoparticles. As shown in Figure 2, the formation of this polaron state is independent of the presence of the halogen ion, but result from the strong CT characteristics of the nanoparticles. In the spectral region around 3 eV, we observe a negative TA signal, which can be associated with transient photobleach (PB); however, it is significantly offset against the ground state absorption maximum at around 2.7 eV. We managed to reproduce the TAS spectra at all delay times for all experiments by assuming a weighted superposition of the charged spectrum, the negative ground state absorption, and an additional Gaussian band (shaded orange, blue and green areas in Figure 2A,C,E). In this spectral model, the relative spectral weights of the contributions, and the Gaussian shape parameters (center energy and width) are the only adjustable parameters. The spectral weights are proportional to the time-resolved concentrations of the corresponding photoexcited states. As shown in Figure 2B,D,F, all three states form within 10 ps and then decay on a 100 ps time scale. However, the ratio between the Gaussian band and the spectrum of the charged state clearly depends on the presence of the halogen ions: for NaCl, this ratio remains constant throughout the measured time range; for NaBr, the ratio slightly increases in favor of the Gaussian band after 200 ps; finally, for NaI, the ratio increases strongly in favor of the Gaussian band starting already after 10 ps.

These observations lead us to identify the Gaussian band with a long-lived state. In fact, in the presence of NaI, we observe a PA band at 2.65 eV as the strongest photoexcitation, see Figure 2E. From the fact that the formation of this state monotonically depends on the atomic mass of the halogen ions, we associate it with the triplet state.

One interesting point is that, as in many reports,[8b,d,e,12] the charge separation of amphiphilic self-assembled photocatalyst is also increased by the salt addition. Aromatic moieties in amphiphilic molecules assemble tightly upon ionic strength change of aqueous solution, consequently inter-molecular charge transfer is increased. However, since this charge transfer showed a very limited lifetime (< ns), it is unlikely to affect the performance of the photocatalyst. Instead, it was confirmed that the addition of iodide clearly promoted ISC, see Figure 2. Comparing the TAS data of with/without iodide (Figure 2), it can be seen that the ratio of triplet/(triplet + charge transfer complex) increases with time in the sample with iodide (Figure 2c). Therefore, we concluded that the formation of the triplet excited state is closely related to the hydrogen production performance through the TAS analysis as well. This triplet state has a sufficiently long lifetime to react with the sacrificial reagent (L-ascorbic acid) by random collision.

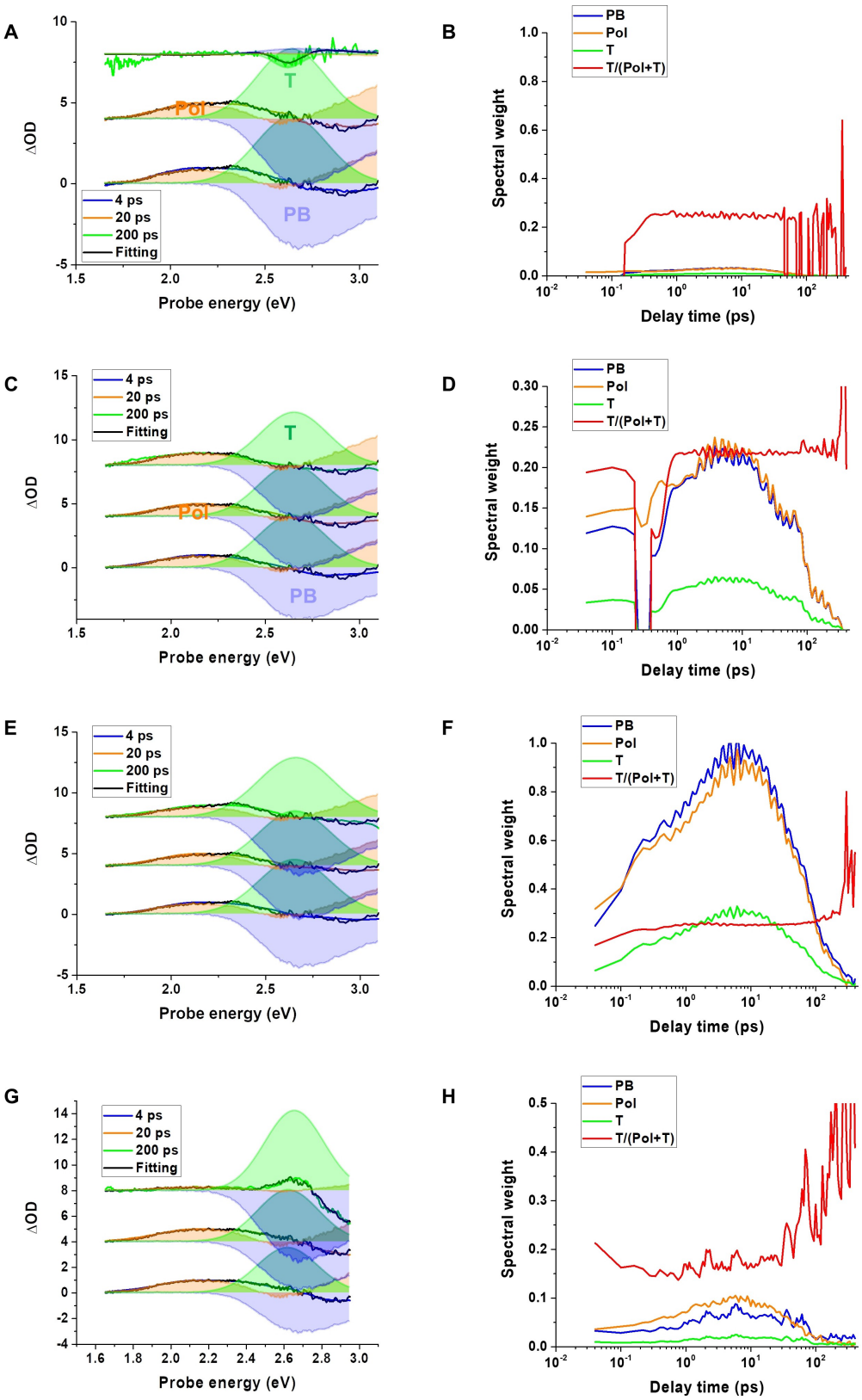


**Figure 2.** Normalized transient absorption spectra and photoexcitation dynamics of the nanoparticles (0.1 mM) A, B) in dimethylsulfoxide (DMSO) solution, C, D) with 0.15 M of NaCl, E, F) NaBr, and G, H) NaI. (PB: photobleach, Pol: polaron, T: triplet state).

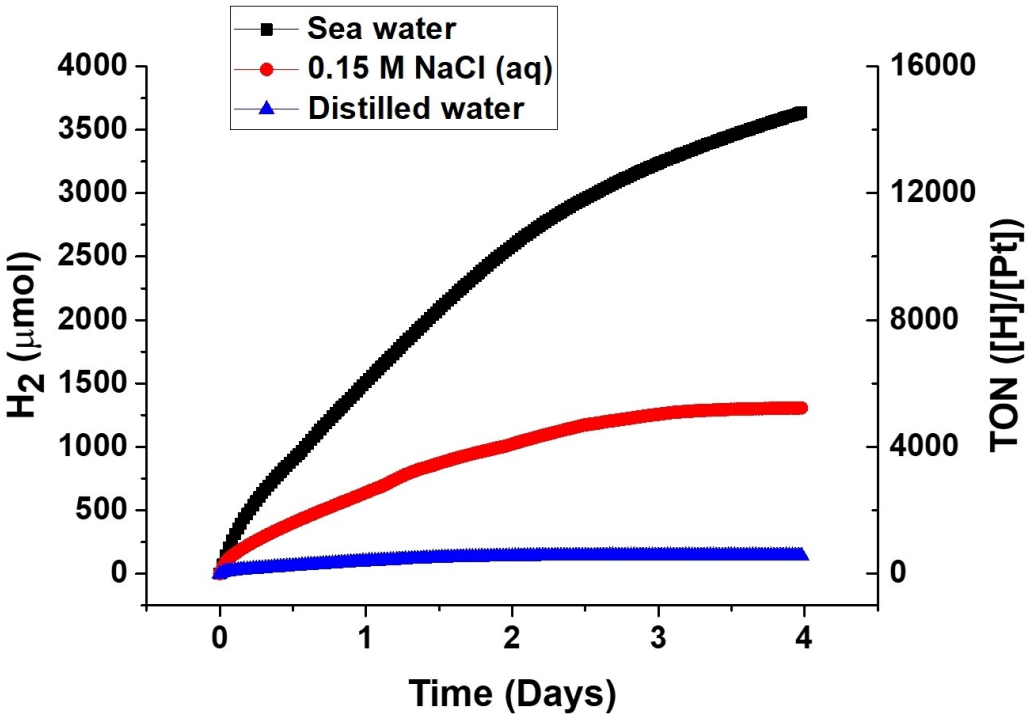


**Figure 3.** HER performances of the supramolecular system in distilled water, 0.15 M of NaCl aqueous solution and seawater under 1 sun condition.

### Probing the Triplet State

The change in the excited state of the self-assembled nanoparticles in aqueous solution upon the addition of halide salt was also examined through a singlet oxygen sensing experiment.[18b,19] For this, the sample was irradiated by a 300 W xenon lamp equipped with a 450 nm band-pass filter, where the sample contained a mixture of the self-assembled nanoparticles and the 'singlet oxygen sensor green' (SOSG) reagent in each aqueous halide solution of 0.15 M concentration. The intensity of light was 3.3 mW/cm$^2$ and the irradiation area was 1 cm$^2$. Irradiation with 450 nm light effectively excites the building block molecule, and the excited species shows a different pathway depending on the additives, i.e. the halide ions. The addition of heavier halide atoms significantly enhanced the ISC of singlet excited molecule, and thus singlet oxygen can be formed subsequently through triplet-triplet energy transfer. Indeed, when iodide was added, a sufficient amount of singlet oxygen was formed to be sensed by SOSG (Figure S2). This is also consistent with the trends observed in the hydrogen evolution experiments (Figure 1D).

### Detecting Excited State Species

We were also able to trace the pathway after photoexcitation through Raman scattering experiments.[20] As illustrated in the UV-Vis spectrum of the building block molecule (Figure 1C), sole information on the ground state of the building block molecule can be obtained when a 785 nm laser is used as an off-resonance Raman scattering source. Therefore, all samples showed similar peaks in the finger-print region (1100–1800 cm$^{-1}$) regardless of the type of additives, see Figure S3. Actually, the positions of peaks (near 1200 cm$^{-1}$ and 1600 cm$^{-1}$) were those predicted by DFT calculations. (Figure S4). The DFT calculations further revealed significant differences between the ground state species compared to the protonated and reduced species, thus confirming that under off-resonant conditions only the building block molecule in its ground state is observed experimentally. On the other hand, when a 325 nm laser is used, i.e. under resonant Raman conditions, information on the excited state is accessible. Interestingly, in this case, the peaks varied depending on the additives, Figure S3. In fact, after the building block molecule was excited, the peak at 1695 cm$^{-1}$ in Figure S3 was apparent only when iodide and ascorbic acid was present. A similar peak position was obtained for the reduced species in the DFT calculations (Figure S4), giving different spectral signatures under resonant conditions compared to the ground state species. From this, we concluded that only when a heavy atom(i.e. iodide) and the electron donor(L-ascorbic acid) are present, photo-reduction was perceived in the resonant Raman scattering measurement.

### Exclusion of Halide Electron Transfer

We then further examined the possibility of halide ion as a source of electrons, as this was reported in literature.[21] First, even when halide salt was added, no hydrogen production was observed without L-ascorbic acid. In addition, X to ligand charge transfer (XLCT, with X = halide) was not confirmed in

the PL spectrum (Figure S5); In fact, in the case of XLCT, when halogen is added, electron transfer occurs to the excited molecule, consequently, the PL should be quenched.[22] Just oppositely, in the current case, when the halide ion was added to the self-assembled nanoparticles, the PL intensity increased. This can most likely be attributed to the fact that, as the ionic strength of the aqueous solution increases, the aggregation of the hydrophobic building block molecule becomes stronger, thus suppressing the non-radiative decay through environmental rigidification.[23] These results indicate that the halide salt does not contribute to the photocatalytic cycle as an electron donor in the present case.

## Stability

In the absence of halide ions, the self-assembled photocatalytic system and sacrificial reagent in water hardly generated hydrogen gas under visible light irradiation. However, the hydrogen production performance increased by adding halide ions. The self-assembled molecular photocatalytic system with iodide and L-ascorbic acid (sacrificial reagent) showed a HER performance of ~8 mmol/g·h without the metal co-catalyst. The TON of the building block molecule for 10 hours reached 100, see Figure 1E. However, without the co-catalyst, the stability of the system was relatively low, which may be due to radical instability as it appears in many organic materials.[8c,24] To investigate the stability of the reduced radical, we assigned first the absorption band of reduced species of the building block molecule. The absorption spectrum of the reduced species of building block molecules was confirmed through an spectro-electrochemical experiment. Distinctive bands are identified in the spectrum of the reduced species, in particular at 600 nm and 400 nm, different from those of the ground state of the building block molecule (Figure S6); similar signatures are identified in the TD-DFT calculations of the reduced species (Figure S15). The 400 nm band is closely related to the degradation mechanism of our self-assembled photocatalytic system. It has been reported that re-excited organic radical anions are highly degradable.[24] For the self-assembled nanoparticles with iodide (triplet enhancing additive) and L-ascorbic acid (electron donor), degradation was indeed observed in the UV-vis spectrum upon irradiation with 400 nm light (Figure S7). On the other hand, this harmful degradation was dramatically reduced by adding Pt co-catalyst, most likely by the rapid draining of the electron from the organic radical ion to Pt (Figure S7). This adapted stability of the organic radical ion by electron relay to Pt has an important influence on hydrogen production. Comparing the experimental results with the 400 nm and the 420 nm long-pass filter, the HER rate of the sample was very similar (Figure S8). While the exposed light intensity to the sample was reduced from 303 mW/cm$^2$ (for a system with a 400 nm long-pass filter) to 293 mW/cm$^2$ (420 nm long-pass filter), and the building block molecule had an absorbance at 400 nm to some extent, both cases showed similar TON. This is most likely attributed to the degradation of radical anion species under 400 nm irradiation. In addition, this degradation effect could also be rationalized by comparing the UV-vis and AQY plots in Figure 1C. In fact, the AQY values of the photocatalytic system at a certain wavelength showed a tendency similar to the UV-vis spectrum of the building block molecule, but with a quite low value at 400 nm. All together, we revealed that in the self-assembled molecular photocatalytic system, the metal co-catalyst not only serves as a catalytic site (Figure 1E, turnover frequency of Pt, $TOF_{Pt}$ ~ 966 h$^{-1}$) but also improves the stability of the photo-active organic material by draining the reduced electrons of the organic system effectively. Such photo-degradation of organic radical ion was also reduced greatly when Pd (Figure S9) and Rh (Figure S10) were used as co-catalysts. However, in these cases, the TOF was significantly lower than when Pt was used ($TOF_{Pd}$ ~ 727 h$^{-1}$, $TOF_{Rh}$ ~ 40 h$^{-1}$).

## Optimization

For a proper evaluation of the self-assembled molecular photocatalytic system,[25] optimization experiments were conducted. While maintaining the amount of the building block molecule, we varied the amounts of Pt or iodide. While 0.65 μmol of the building block molecule in a 0.15 M of NaI aqueous solution (300 mg of NaI in 13 mL of solution) was used, a sample with 0.25 μmol of Pt produced the maximized hydrogen gas for 10 hours (about 3 mmol, Figure S11). When a smaller amount of Pt was used, $TON_{Pt}$ was over 10,000 for the first few hours, but then decreased rapidly. In this case, the amount of Pt was not enough to effectively depopulate the radicals. When more than 0.25 μmol of Pt was used, $TON_{Pt}$ for 10 hours decreased again. This decrease was most likely caused by too much scattering of Pt colloids which interferes with the photo-active organic molecules' ability to absorb light. On the other hand, when varying the concentration of iodide from 0 M to 0.26 M, both $TON_{Pt}$ and $TOF_{Pt}$ increased proportionally with the concentration of iodide in the self-assembled molecular photocatalytic system. With 0.65 μmol of the building block molecule and 0.5 μmol of Pt, the self-assembled molecular photocatalyst in 0.26 M of NaI aqueous solution produced the largest hydrogen gas (2.4 mmol, Figure S12).

## Photocatalytic Activity in Seawater

The results from using external halide ions in the photocatalytic water splitting system have opened new possibilities for the use of seawater, the most abundant resource on earth. In addition, we used a solar simulator as a light source to create a more practical photocatalytic condition. Although the chloride ion showed the weakest effect among the halogen additives in our experiment due to its relatively small molecular weight, seawater contains a much higher concentration of chloride than that used in our experiments. We collected seawater directly from a coast located in Incheon, Korea for use in experiments. In general, 1 kg of seawater from that location contains about 33 g of salts, including NaCl, $MgCl_2$, and $Na_2SO_4$.

Therefore, the seawater will contain a much higher amount of NaCl than the 0.15 M NaCl aqueous solution (about 8.8 g of NaCl in 1 kg of solution) used in the experiments ascribed above. Consequently, the sample prepared by using seawater showed much larger $TOF_{Pt}$ (577 $h^{-1}$), $TON_{Pt}$ during 24 hours (6035), and during 4 days (14542) than the self-assembled molecular photocatalyst in distilled water ($TOF_{Pt}$ ~ 68 $h^{-1}$, $TONF_{Pt}$ ~ 386) as well as the self-assembled molecular photocatalyst in 0.15 M NaCl. ($TOF_{Pt}$ ~ 380 $h^{-1}$, $TONF_{Pt}$ ~ 2557, Figure 3) AQY of the sample using seawater was also following the UV-vis absorption spectra of the building block molecule, and was highest at 500 nm (3.8%, Figure S13). Since many efforts have been made to utilize seawater in the field of water splitting,[26] it is very encouraging that our system showed better performance (over 37 times better $TON_{Pt}$) upon solar simulator irradiation than distilled water.

## Conclusions

In summary, we designed a novel octupolar molecule as an effective building block for self-assembled molecular hydrogen evolution catalysis. In aqueous solution, the molecules self-assemble into positively charged nanoparticles with about 100 nanometers in diameter, showing good visible light absorption, and providing interactions with negatively charged additives. We upgraded its photocatalytic hydrogen evolution performance by using halide additives, and analyzed the effects of the additives to elucidate the underlying photocatalytic mechanism. The optimized system (0.65 μmol of the building block molecule and 0.5 μmol of Pt with 0.15 M of iodide additives) showed good performance with over 20,000 $TON_{Pt}$ and 9.8% of AQY (at 500 nm). To investigate the mechanism of halides additives, we analyzed each photocatalytic step by using TA and Raman spectroscopy, as well as singlet oxygen sensing experiments, complemented by computational analysis. Combining the mechanistic study and the performance evolution upon halide addition, we concluded: that 1) the singlet excited state lifetime of the building block ($<$ ns) is insufficient to be reduced by the sacrificial reagent, 2) the presence of halides effectively induce intersystem crossing to the triplet excited state by a heavy atom effect 3) prolonged lifetime of the triplet state effectively promotes the desirable photocatalytic cycle. Further, we observed that the performance enhancement induced by additives increased by atomic weight or concentration of the additives. Interestingly, this observation implied that seawater, the most abundant resource on the earth, has advantages over distilled water as a proton source of our photocatalytic system. As a result, we successfully implemented seawater-based water-splitting system with our self-assembled photocatalyst. Remarkably, our self-assembled photocatalyst produced 3.6 mmol of $H_2$ gas by utilizing 13 ml of natural seawater under 1 sun condition.

## Acknowledgements

*This work at Seoul National University was supported by the Basic Science Research Program through the NRF funded by the Ministry of Science, ICT and Future Planning (2017R1E1A1A01075372). The work in Madrid was supported by the Spanish Science Ministry (MINECO-FEDER projects CTQ2017-87054, SEV-2016-0686, and MICINN project CEX2020-001039-S) and by the Campus of International Excellence (CEI) UAM + CSIC.*

## Conflict of Interest

The authors declare no conflict of interest.

## Data Availability Statement

The data that support the findings of this study are available from the corresponding author upon reasonable request.

**Keywords:** hydrogen evolution · intersystem crossing · photocatalysis · self-assembly · water splitting

[1] a) L. Yuan, C. Han, M. Q. Yang, Y. J. Xu, *Int. Rev. Phys. Chem.* **2016**, *35*, 1–36; b) J. R. McKone, N. S. Lewis, H. B. Gray, *Chem. Mater.* **2013**, *26*, 407–414.
[2] a) D. N. Tritton, G. B. Bodedla, G. Tang, J. Zhao, C.-S. Kwan, K. C.-F. Leung, W.-Y. Wong, X. Zhu, *J. Mater. Chem. A* **2020**, *8*, 3005–3010; b) D. N. Tritton, F.-K. Tang, G. B. Bodedla, F.-W. Lee, C.-S. Kwan, K. C.-F. Leung, X. Zhu, W.-Y. Wong, *Coord. Chem. Rev.* **2022**, *459*, 214390.
[3] T. Takata, J. Jiang, Y. Sakata, M. Nakabayashi, N. Shibata, V. Nandal, K. Seki, T. Hisatomi, K. Domen, *Nature* **2020**, *581*, 411–414.
[4] a) J. Warnan, E. Reisner, *Angew. Chem. Int. Ed.* **2020**, *59*, 17344–17354; *Angew. Chem.* **2020**, *132*, 17496–17506; b) S. Bellani, M. R. Antognazza, F. Bonaccorso, *Adv. Mater.* **2019**, *31*, 1801446.
[5] a) L. Wang, R. Fernandez-Teran, L. Zhang, D. L. Fernandes, L. Tian, H. Chen, H. Tian, *Angew. Chem. Int. Ed.* **2016**, *55*, 12306–12310; *Angew. Chem.* **2016**, *128*, 12494–12498; b) P. B. Pati, G. Damas, L. Tian, D. L. A. Fernandes, L. Zhang, I. B. Pehlivan, T. Edvinsson, C. M. Araujo, H. N. Tian, *Energy Environ. Sci.* **2017**, *10*, 1372–1376; c) Y. Bai, L. Wilbraham, B. J. Slater, M. A. Zwijnenburg, R. S. Sprick, A. I. Cooper, *J. Am. Chem. Soc.* **2019**, *141*, 9063–9071.
[6] a) X. Wang, L. Chen, S. Y. Chong, M. A. Little, Y. Wu, W. H. Zhu, R. Clowes, Y. Yan, M. A. Zwijnenburg, R. S. Sprick, A. I. Cooper, *Nat. Chem.* **2018**, *10*, 1180–1189; b) H. S. Jena, C. Krishnaraj, S. Parwaiz, F. Lecoeuvre, J. Schmidt, D. Pradhan, P. Van Der Voort, *ACS Appl. Mater. Interfaces* **2020**, *12*, 44689–44699; c) T.-X. Wang, H.-P. Liang, D. A. Anito, X. Ding, B.-H. Han, *J. Mater. Chem. A* **2020**, *8*, 7003–7034; d) W.-J. Xiao, Y. Wang, W.-R. Wang, J. Li, J. Wang, Z.-W. Xu, J. Li, J. Yao, W.-S. Li, *Macromolecules* **2020**, *53*, 2454–2463; e) S. Luo, Z. Zeng, G. Zeng, Z. Liu, R. Xiao, P. Xu, H. Wang, D. Huang, Y. Liu, B. Shao, Q. Liang, D. Wang, Q. He, L. Qin, Y. Fu, *J. Mater. Chem. A* **2020**, *8*, 6434–6470; f) S. Zhang, G. Cheng, L. Guo, N. Wang, B. Tan, S. Jin, *Angew. Chem. Int. Ed.* **2020**, *59*, 6007–6014; *Angew. Chem.* **2020**, *132*, 6063–6070; g) X. Gao, C. Shu, C. Zhang, W. Ma, S.-B. Ren, F. Wang, Y. Chen, J. H. Zeng, J.-X. Jiang, *J. Mater. Chem. A* **2020**, *8*, 2404–2411; h) X. Zhou, Y. Liu, Z. Jin, M. Huang, F. Zhou, J. Song, J. Qu, Y.-J. Zeng, P.-C. Qian, W.-Y. Wong, *Adv. Sci.* **2021**, *8*, 2002465.
[7] G. Pirotte, J. Kesters, P. Verstappen, S. Govaerts, J. Manca, L. Lutsen, D. Vanderzande, W. Maes, *ChemSusChem* **2015**, *8*, 3228–3233.
[8] a) O. Dumele, J. Chen, J. V. Passarelli, S. I. Stupp, *Adv. Mater.* **2020**, *32*, 1907247; b) A. S. Weingarten, R. V. Kazantsev, L. C. Palmer, M. McClendon, A. R. Koltonow, A. P. Samuel, D. J. Kiebala, M. R. Wasielewski, S. I. Stupp, *Nat. Chem.* **2014**, *6*, 964–970; c) H. J. Lee, J. Kim, A. Abudulimu, J. Cabanillas-Gonzalez, P. C. Nandajan, J. Gierschner, L. Luer, S. Y. Park, *J.*

*Phys. Chem. C* **2020**, *124*, 6971–6978; d) A. S. Weingarten, R. V. Kazantsev, L. C. Palmer, D. J. Fairfield, A. R. Koltonow, S. I. Stupp, *J. Am. Chem. Soc.* **2015**, *137*, 15241–15246; e) X. Y. Yang, Z. C. Hu, Q. W. Yin, C. Shu, X. F. Jiang, J. Zhang, X. H. Wang, J. X. Jiang, F. Huang, Y. Cao, *Adv. Funct. Mater.* **2019**, *29*, 1808156; f) M. C. Nolan, J. J. Walsh, L. L. E. Mears, E. R. Draper, M. Wallace, M. Barrow, B. Dietrich, S. M. King, A. J. Cowan, D. J. Adams, *J. Mater. Chem. A* **2017**, *5*, 7555–7563; g) K. Kong, S. Zhang, Y. Chu, Y. Hu, F. Yu, H. Ye, H. Ding, J. Hua, *Chem. Commun.* **2019**, *55*, 8090–8093.

[9] E. Baranoff, F. Nakatsu, Y. Kamikawa, H. B. Liu, M. Moriyama, K. Kumazawa, M. Yoshizawa, M. Fujita, T. Kato, *55th SPSJ Annual Meeting, Vol. 55*, 1 ed., Nagoya **2006**, p. 688.

[10] a) Z. Zhang, Y. Zhu, X. Chen, H. Zhang, J. Wang, *Adv. Mater.* **2019**, *31*, 1806626; b) G. B. Bodedla, J. Huang, W.-Y. Wong, X. Zhu, *ACS Appl. Nano Mater.* **2020**, *3*, 7040–7046.

[11] a) H. Yang, X. Li, R. S. Sprick, A. I. Cooper, *Chem. Commun.* **2020**, *56*, 6790–6793; b) J. Kosco, M. Bidwell, H. Cha, T. Martin, C. T. Howells, M. Sachs, D. H. Anjum, S. Gonzalez Lopez, L. Zou, A. Wadsworth, W. Zhang, L. Zhang, J. Tellam, R. Sougrat, F. Laquai, D. M. DeLongchamp, J. R. Durrant, I. McCulloch, *Nat. Mater.* **2020**, *19*, 559–565.

[12] a) A. S. Weingarten, A. J. Dannenhoffer, R. V. Kazantsev, H. Sai, D. Huang, S. I. Stupp, *J. Am. Chem. Soc.* **2018**, *140*, 4965–4968; b) N. J. Hestand, R. V. Kazantsev, A. S. Weingarten, L. C. Palmer, S. I. Stupp, F. C. Spano, *J. Am. Chem. Soc.* **2016**, *138*, 11762–11774.

[13] a) O. Maury, H. Le Bozec, *Acc. Chem. Res.* **2005**, *38*, 691–704; b) H. M. Kim, M. S. Seo, S.-J. Jeon, B. R. Cho, *Chem. Commun.* **2009**, 7422–7424; c) J. Zyss, I. Ledoux, *Chem. Rev.* **1994**, *94*, 77–105; d) D. Cvejn, E. Michail, I. Polyzos, N. Almonasy, O. Pytela, M. Klikar, T. Mikysek, V. Giannetas, M. Fakis, F. Bureš, *J. Mater. Chem. C* **2015**, *3*, 7345–7355; e) H. M. Kim, B. R. Cho, *J. Mater. Chem.* **2009**, *19*, 7402–7409.

[14] J. Xu, C. Yang, S. Bi, W. Wang, Y. He, D. Wu, Q. Liang, X. Wang, F. Zhang, *Angew. Chem. Int. Ed.* **2020**, *59*, 23845–23853; *Angew. Chem.* **2020**, *132*, 24053–24061.

[15] H. J. Lee, H. J. Kim, E. C. Lee, J. Kim, S. Y. Park, *Chem. Asian J.* **2018**, *13*, 390–394.

[16] S. Wang, X. Wang, S. P. Jiang, *Phys. Chem. Chem. Phys.* **2011**, *13*, 6883–6891.

[17] a) M. Bartolini, V. Gombac, A. Sinicropi, G. Reginato, A. Dessì, A. Mordini, J. Filippi, T. Montini, M. Calamante, P. Fornasiero, L. Zani, *ACS Appl. Energ. Mater.* **2020**, *3*, 8912–8928; b) G. Li, M. F. Mark, H. Lv, D. W. McCamant, R. Eisenberg, *J. Am. Chem. Soc.* **2018**, *140*, 2575–2586; c) S. Rajasekar, V. Tiwari, U. Srivastva, S. Holdcroft, *ACS Appl. Energ. Mater.* **2020**, *3*, 8988–9001.

[18] a) J. Lu, B. Pattengale, Q. Liu, S. Yang, W. Shi, S. Li, J. Huang, J. Zhang, *J. Am. Chem. Soc.* **2018**, *140*, 13719–13725; b) H. Wang, S. Jiang, W. Liu, X. Zhang, Q. Zhang, Y. Luo, Y. Xie, *Angew. Chem. Int. Ed.* **2020**, *59*, 11093–11100; *Angew. Chem.* **2020**, *132*, 11186–11193.

[19] a) A. Prasad, M. Sedlarova, P. Pospisil, *Sci. Rep.* **2018**, *8*, 13685; b) C. Flors, M. J. Fryer, J. Waring, B. Reeder, U. Bechtold, P. M. Mullineaux, S. Nonell, M. T. Wilson, N. R. Baker, *J. Exp. Bot.* **2006**, *57*, 1725–1734.

[20] H. Sun, I. H. Öner, T. Wang, T. Zhang, O. Selyshchev, C. Neumann, Y. Fu, Z. Liao, S. Xu, Y. Hou, A. Turchanin, D. R. T. Zahn, E. Zschech, I. M. Weidinger, J. Zhang, X. Feng, *Angew. Chem. Int. Ed.* **2019**, *58*, 10368–10374; *Angew. Chem.* **2019**, *131*, 10476–10482.

[21] a) J. X. Li, C. Ye, X. B. Li, Z. J. Li, X. W. Gao, B. Chen, C. H. Tung, L. Z. Wu, *Adv. Mater.* **2017**, *29*, 1606009; b) G. Zhang, G. Li, Z.-A. Lan, L. Lin, A. Savateev, T. Heil, S. Zafeiratos, X. Wang, M. Antonietti, *Angew. Chem. Int. Ed.* **2017**, *56*, 13445–13449; *Angew. Chem.* **2017**, *129*, 13630–13634.

[22] C. Nguyen, K. O. Zahir, *J. Environ. Sci. Health Part B* **1999**, *34*, 1–16.

[23] J. Gierschner, J. Shi, B. Milián-Medina, D. Roca-Sanjuán, S. Varghese, S. Park, *Adv. Opt. Mater.* **2021**, *9*, 2002251.

[24] T. Shimidzu, T. Iyoda, Y. Koide, *J. Am. Chem. Soc.* **1985**, *107*, 35–41.

[25] M. Qureshi, K. Takanabe, *Chem. Mater.* **2017**, *29*, 158–167.

[26] a) J. Liu, Y. Liu, N. Y. Liu, Y. Z. Han, X. Zhang, H. Huang, Y. Lifshitz, S. T. Lee, J. Zhong, Z. H. Kang, *Science* **2015**, *347*, 970–974; b) Y. Kuang, M. J. Kenney, Y. Meng, W.-H. Hung, Y. Liu, J. E. Huang, R. Prasanna, P. Li, Y. Li, L. Wang, M.-C. Lin, M. D. McGehee, X. Sun, H. Dai, *Proc. Natl. Acad. Sci. USA* **2019**, *116*, 6624–6629; c) J. Zheng, Y. Zhao, H. Xi, C. Li, *RSC Adv.* **2018**, *8*, 9423–9429.

Manuscript received: June 28, 2022
Revised manuscript received: August 29, 2022
Accepted manuscript online: September 12, 2022
Version of record online: ■■, ■■■

# RESEARCH ARTICLES

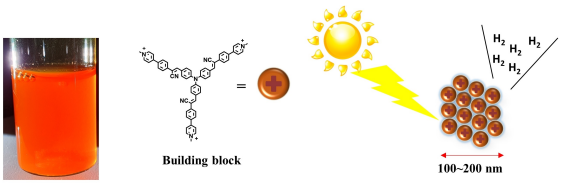


*Dr. H.-J. Lee, Dr. A. Abudulimu, J. C. Roldao, H. Nam, Prof. Dr. J. Gierschner*, Prof. Dr. L. Lüer*, Prof. Dr. S. Y. Park**



**An octupolar molecule** with excellent visible light absorption and strong intramolecular charge transfer characteristics was designed and synthesized. In aqueous solution, the molecules self-assemble into positively charged nanoparticles. The optimized self-assembled system (composed of nanoparticles with platinum and halide additives) reached a maximum hydrogen evolution rate of 460 mmol/g·h.